frontiers | Frontiers in Environmental Science

TYPE Original Research
PUBLISHED 03 October 2022
DOI 10.3389/fenvs.2022.943776

OPEN ACCESS

EDITED BY
Belkis Sulbaran-Rangel,
University of Guadalajara, Mexico

REVIEWED BY
Patricia Ponce Peña,
Juárez University of the State of Durango, Mexico
Eddy Sánchez-DelaCruz,
Tecnológico Nacional de México, Mexico

*CORRESPONDENCE
Claudia A. Aguilar,
caguilar@pampano.unacar.mx

SPECIALTY SECTION
This article was submitted to Water and Wastewater Management, a section of the journal Frontiers in Environmental Science

RECEIVED 14 May 2022
ACCEPTED 29 August 2022
PUBLISHED 03 October 2022

CITATION
Aguilar CA, de la Cruz A, Montalvo C, Ruiz-Marín A, Oros-Ruiz S, Figueroa-Ramírez SJ, Abatal M, Anguebes F and Córdova-Quiroz V (2022), Effect of kinetics on the photocatalytic degradation of acetaminophen and the distribution of major intermediate with anatase-Ag synthesized by sol gel under visible irradiation.
Front. Environ. Sci. 10:943776.
doi: 10.3389/fenvs.2022.943776

Effect of kinetics on the photocatalytic degradation of acetaminophen and the distribution of major intermediate with anatase-Ag synthesized by sol gel under visible irradiation

Claudia A. Aguilar[1]*, Alberto de la Cruz[1], Carlos Montalvo[1], Alejandro Ruiz-Marín[1], Socorro Oros-Ruiz[2], Sandra J. Figueroa-Ramírez[3], Mohamed Abatal[3], Francisco Anguebes[1] and Victor Córdova-Quiroz[1]

[1]Faculty of Chemistry, Autonomous University of Carmen, Campeche, Mexico, [2]Department of Chemistry, Iztapalapa Unit, Autonomous Metropolitan University, Mexico City, Mexico, [3]Faculty of Engineering, Autonomous University of Carmen, Campeche, Mexico

The degradation of acetaminophen (ACET) was studied with TiO_2-Ag catalysts, whose predominant crystalline phase was anatase, synthesized by the sol–gel method and doped by photo-deposition under UV radiation with silver particles. The catalyst was characterized by energy dispersive X-ray fluorescence (EDXRF) and X-ray diffraction (DRX). The acetaminophen degradation was determined by high-performance liquid chromatography (HPLC) and total organic carbon (TOC). The reaction behavior was studied under the Langmuir–Hinshelwood (LH-HW) equation and in a TOC-based model. With the experimental data, mass balances were performed to introduce the constants (reaction and adsorption kinetics) to the LH-HW equation. With the analysis of the generation and consumption behavior of the organic intermediate compounds (OI), coupled differential equations were generated, which express the degradation and formation-consumption behavior. The kinetic constants were obtained by nonlinear regression using the Levenberg–Marquardt equation. The results show high removal percentages, and the behavior of the experimental data is assumed to fit the LH-HW equation. The analysis of the organic intermediates by solid phase micro-extraction (SPE), HPLC and gas chromatography (CG-MS), shows that the transformation is feasible under the formation of nitro-aromatic derivatives and hydroxylated species.

KEYWORDS

anatase-Ag powder, visible light, acetaminophen, kinetic study, organic intermediates

Introduction

Recent studies have reported the presence of organic molecules such as pharmaceutical residues in the continental waters of European, Asian, and North American countries (Wilkinson et al., 2022); although these data are scarce and present variations in their sampling methods and analytical techniques, which makes it difficult to establish a comparison and a real situation, there is evidence of their presence and increase in groundwater, rivers, and lakes.

Pharmaceutical residues are considered "emerging contaminants." These are molecules that are present in low concentrations of the order of ppm or ppb, or whose characteristics are still partly unknown (Chan et al., 2022). Acetaminophen, due to its excessive use and high accessibility in the world, is an emerging contaminant of interest (Chopra and Kumar, 2020). Also, its waste ends up in rivers, lakes, and treatment plants.

The presence of acetaminophen in biological treatment systems causes inhibition in the growth of microorganisms, which decreases the efficiency of the processes (Bedner and Maccrehan, 2006) and is toxic to algae such as *Dapnia magna* and *Tetrahymena pyriformes* in wastewater and surface water effluents (Castro et al., 2015). Chopra and Kumar (2020) identified bacterial strains of *Bacillus sp.*, *Enterococcus sp.*, and *Staphylococcus spp.* as being capable of tolerating and degrading acetaminophen and its secondary products up to a certain concentration. However, the continuous injection of different organic molecules into water effluents can put the health of ecosystems at risk and reduce the efficiency of treatment systems.

Different methods have been developed to degrade acetaminophen including electrocoagulation processes (Kumari and Naresh, 2021), Fenton and its variants, Cu/Fe compounds, Fe III, and complexes of glutamic and lactic acids (Hurtado et al., 2019; Benssassi et al., 2021); processes based on the generation of oxidizing species with the use of H_2O_2, O_3, and UV light (Bavasso et al., 2020; Dibene et al., 2021); and other techniques with different principles such as capillary electrophoresis using ZnO films (Hernández et al., 2021).

The use of catalysts for the degradation of acetaminophen occupies an important place in these processes and offers advantages by chemically transforming the organic structure. Examples of these processes are those developed with Ag-Ag_2O assisted by microwaves (Jannatun and Ufana, 2020) or with co-doped bismuth and Cu catalysts under visible irradiation (Abbas et al., 2022). Silver nanoparticles and ZnO and CuO nanorods (Al-Gharibi et al., 2021; Aminzadeh et al., 2021) are just some of the recent developments, although these studies present promising results.

Titanium dioxide (TiO_2) is a catalyst used in the removal of acetaminophen whether doped, supported, or forming nanocomposites. Ziylan-Yavas and Ince (2016) studied the elimination of acetaminophen by catalytic oxidation with ultrasound processes and UV radiation with Pt immobilized on TiO_2, which facilitated the separation of charges. When TiO_2 is supported on a porous substrate such as zeolite with sol–gel processes, the percentage of acetaminophen degradation is high (≥90%). Hydroxylation and hydrolysis are the initial paths of transformation (Chang et al., 2015). TiO_2 has been used in photocatalysis due to its excellent characteristics (Janus and Morawski, 2007; Jallouli et al., 2017; Moma and Baloyi., 2018). Unlike the catalysts synthesized by the sol–gel method, the crystalline phases of the material can be controlled. The synthesis process makes the difference with respect to other commercial titanium-based materials. The addition of Ag as a dopant under the photo-deposition method with UV radiation is capable of reducing the oxidation state of the metallic silver as a whole with controlled calcination (Wahyuni and Roto 2018).

The structure of the catalyst has an important role in the final results. Borras-Ferris et al. (2019) used TiO_2 nanotubes obtained by electrochemical anodization processes with the predominant anatase phase; in their results, the degradation of acetaminophen was related to hydrodynamic conditions. Other supports have shown high efficiency when coupled to TiO_2. Gomez-Solís et al. (2021) used flexible graphene composites decorated with TiO_2 nanoparticles (Ni@ TiO2:W) for the degradation of acetaminophen with solar radiation.

Catalysts doped with metallic particles perform better under visible radiation (Seery et al., 2007). Ag particles or others, such as Cu, Au, and Pt, function as scavengers for the electrons that come from the valence band and make the charge separation process efficient; this avoids recombination processes that generate neutral centers. The incorporation of Ag in TiO_2 improves its absorption capacity in the visible light range, which is not possible with commercial catalysts that are only active in the ultraviolet light range. Furthermore, the surface plasmon resonance (SPR) effect of Ag on the photocatalyst surface also facilitates the photocatalytic reaction (Yong et al., 2022).

The objective of this study was to synthesize a TiO_2-Ag catalyst from an alkoxide precursor for the formation of anatase powders, doping them with silver particles, and using this catalyst for the degradation of acetaminophen in the presence of visible light. To evaluate the effects on the reaction kinetics under different kinetic models and to identify the mechanisms of the probable routes of transformation of the major compounds.

Experimental setup

Materials and equipment

For the synthesis of anatase powders, the precursors of titanium butoxide (CAS 5593-70-4) and 1-butanol (71-36-3) were used. For the degradation tests and identification of organic intermediates, acetaminophen ACET (CAS 103-90-2) and standards of 4-aminophenol AP (CAS 123-30-8), hydroquinone HQ (CAS 123-31-9), p-benzoquinone BQ (CAS 106-51-4), and 1,2-hydroxybenzene

or catechol CT (120-80-9) were used. All these reagents are of the Aldrich brand. For the doping of the anatase powders, silver nitrate precursor salts (CAS 7761-88-8) from the Merck brand were used.

For evaluation of reaction samples by HPLC, an Agilent 1100 equipment adapted with a quaternary pump and a Zorbax (C-18) column was used. The mobile phase was prepared using the gradient function of the equipment, with a mixture of water HPLC grade from the Merck brand and methanol spectroscopic grade (CAS 67-56-1) from the Fischer Scientific brand. Prior to analysis, reaction samples were passed through a 0.22 μm cellulose acetate filter media (Millipore Corp., Bedford, MA).

For the extraction of the organic phase, solid phase microextraction (SPE) was used with LiChrolut® EN cartridges (40–120 μm) of the Merck brand. This is suitable for samples with polar organic compounds, due to its specific surface area (1,200 m^2/g according to the BET method), which offers excellent adsorption capacity for polar organic substances, such as phenols, nitro-aromatic compounds, and anilines. Chromatographic analysis (GC-MS) was performed using an Agilent Model 6890 equipped with a Model 5973N Mass Detector and a 29 m × 0.25 mm × 0.25 μm HP-5MS column.

For the monitoring of total organic carbon (TOC), a Shimadzu model 5000A analyzer was used, and potassium biphthalate (CAS 877-24-7) and sodium bicarbonate (CAS 144-55-8) standards both from the Nakalai Tesque brand were used for calibration.

Silver-doped anatase powders were characterized by X-ray diffraction (DRX) using a Bruker D2 phaser and by energy dispersive X-ray fluorescence (EDXRF) using a JEOL, JSX-100s.

Preparation and doping of the catalyst

For the synthesis of the catalyst, 24.34 g of titanium butoxide were mixed with ¾ of butanol under continuous stirring at 250 rpm. After 1 h of reaction (and keeping up the stirring), the remaining ¼ part of the alcohol and the 7.8 g of water were added by slow dripping. The mixture was prepared in an OS20—pro-equipment of the Science Med Finland Technology brand; the reaction equipment operates at total reflux. The gel obtained remained at rest for 24 h, and then it was dried at 120°C for 12 h and finely calcined at 550°C for 5 h.

To carry out the photo-deposition of silver, $AgNO_3$ precursor salts were used. The amount of silver nitrate to be used for 0.5 g of catalyst was established according to Eqs 1–3.

$$\text{Ag particles}\frac{\text{surface area of the support}}{\text{particle area}} = \frac{25\ m^2}{6.5144 \times 10^{-20} m^2} = 3.84 \times 10^{20} \quad (1)$$

$$\text{Ag weight} = \left(3.84 \times 10^{20}\text{particles}\right)\left(107.87\frac{g}{mol}\right) \times \left(\frac{1\ mol}{6.023 \times 10^{23}\text{particles}}\right) = 0.0687g \quad (2)$$

$$AgNO_3\text{weight} = \frac{(\text{Ag weight})(\text{molecular weight of } AgNO_3)}{(\text{molecular weight of Ag})}. \quad (3)$$

Initially, the solution remains 1 h in the dark phase to favor the adsorption processes. After that period, it remains for 5 h with the irradiation of 4 UV lamps (λmax = 365 nm, Cole-Parmer E-09815-55); the water is removed by vacuum filtration followed by a drying process at 120°C for 5 h and calcination at 550°C for 5 h, and this is a fundamental process to define the physical and chemical characteristics (Behpour et al., 2010).

Photodegradation and photoactivity

A volume of 250 ml was used for each test. At different concentration ranges in mg/l of ACET, a Bach-type reactor with a catalyst mass of 2 g/l was used. The reaction was carried out under the continuous injection of oxygen with a concentration of 100 cm^3/min. The reaction samples were analyzed by HPLC and TOC.

Results and discussion

Catalyst characterization

Figure 1 shows the DRX pattern of the synthesized catalyst. It can be seen that the predominant phase is anatase, and the synthesis of the catalyst was carried out under the control of the calcination temperature at 550°C, propitiating that the predominant phase is the anatase. This crystalline phase has been considered the most active in light-accelerated catalysis processes. Sharp peaks show stability in the crystalline phase of the semiconductor.

When DRX analytical techniques do not allow to visualize the fractions of the elemental composition, it is possible to use EDXRF. Under these techniques, it was possible to know the elemental composition of the synthesized material, being the percentage of silver deposited 1.17% with respect to the total mass of the solid material (Figure 2). The catalyst synthesis process under UV irradiation makes it possible to control the oxidation states of the deposited metallic silver, which is reduced and favors the efficiency of the catalyst in these processes (Behpour et al., 2010).

Similar percentages of the dopant have been used in other studies. Seery et al. (2007) used percentages of Ag between 1–3% in relation to TiO_2, obtaining high values of rhodamine removal in the range of visible light with pre-irradiated catalysts.

Aguilar et al. (2019) used commercial TiO_2 doped with Ag (5–15%). In their results, it is shown that the mass of the dopant neither has no influence on the increase in the absorption capacity of the catalyst in the region of visible light nor on the decrease in the band gap of the catalyst. The conversion percentages were higher than 80% when using the lowest percentage of Ag deposited in the TiO_2.

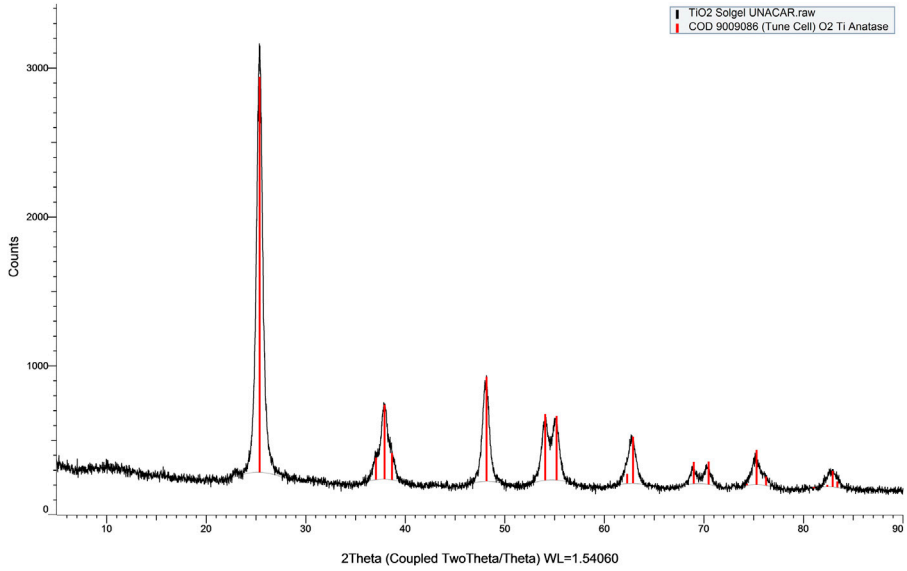

FIGURE 1
X-ray diffraction pattern (DRX) of the synthesized catalyst (TiO_2-Ag).

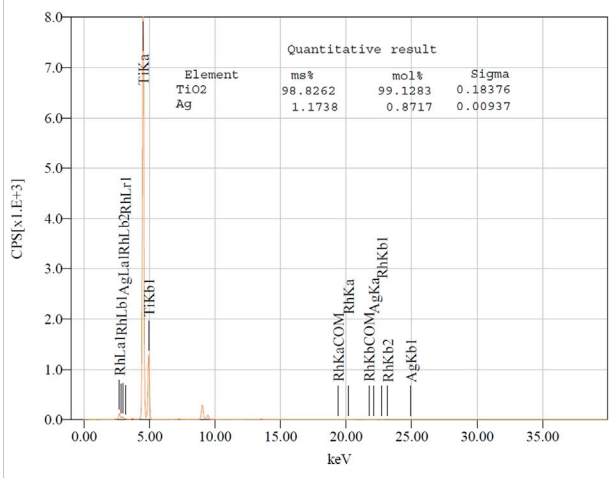

FIGURE 2
Energy dispersive X-ray fluorescence (EDXRF) of the TiO_2-Ag catalyst synthesized by the sol gel method.

Kőrösi et al. (2008) used percentages of Ag between 0.1 and 1% in relation to the mass of TiO_2 with excellent conversion percentages.

Kinetics of photocatalytic degradation

When there is the presence of a catalyst, the chemical reaction can be evaluated under the model of heterogeneous catalysis. In this process, the catalyst is thermally activated; in heterogeneous photocatalysis, the catalyst is activated by energy photons (García-Lopez et al., 2019).

Photocatalysis reactions (Guo et al., 2019) occur when an electron from the valence band jumps to the conduction band, generating a photo-hole in the semiconductor due to the effect of an external energy source. When there are species in the medium that are capable of sequestering the electron, such as oxygen or metal ions, the process is optimized. In the opposite case, charge recombination occurs, which affects the global efficiency. This is the objective of doping a semiconductor with metal ions, with the additional advantage that the changes promoted on the surface of the catalyst make it possible for it to be active in visible light.

The results of several studies show that the degradation rates by photocatalysis fit the LH-HW model (Eq. 4) (Kabra et al., 2004; Yang et al., 2008; Yang et al., 2010).

$$-r_{ACET} = -\frac{dC_{ACET}}{dt} = \frac{K_1 C_{ACET}}{1 + K_2 C_{ACET} + \sum K_i C_{OI}} \quad (4)$$

The above mentioned equation shows the term of $\sum K_i C_{OI}$ which corresponds to the kinetic constant by the concentration of organic intermediates. For the estimation of the OI, as a global mass, a correction of the data is performed based on the TOC, as suggested by Eq. 5, and the milli-equivalents of carbon in the HPLC results are determined. Finally, a mass balance is performed on a carbon basis according to Eq. 6.

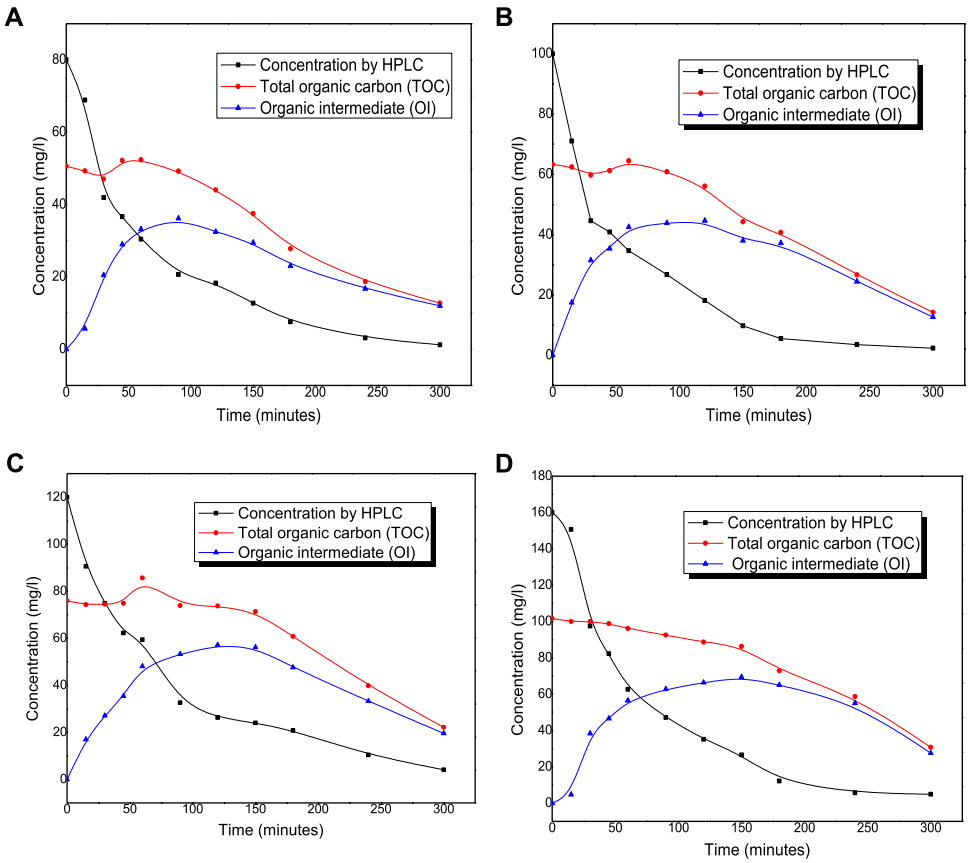

FIGURE 3
Distribution profile of ACET degradation from the experimental data followed by HPLC and of the mineralization by TOC also shows the curves of the estimated IO generation and consumption obtained by mass balances. **(A)** C_{ACET} = 80 mg/l, **(B)** C_{ACET} = 100 mg/l, **(C)** C_{ACET} = 120 mg/l, and **(D)** C_{ACET} = 160 mg/l. In all cases, the degradation conditions were as follows: reaction volume = 250 ml; oxygen concentration = 100 cm^3/min; catalyst mass = 2 gr/l; four commercial visible light lamps were irradiated.

$$TOC_{[mg/l]t=t} = TOC_{[mg/l]t=0}\left[\frac{TOC_{[mg/l]t=t}}{TOC_{[mg/l]t=0}}\right]_{experimental} \quad (5)$$

$$C_{OI} = TOC_{(mg/l)} - HPLC_{(mg/l)} \quad (6)$$

For the total estimation of the term of $\sum K_i C_{OI}$, all organic intermediates are assumed to have the same constant. This is because they have short lifetimes, so it is reasonable to consider that they can be evaluated under the same kinetic constant.

$\sum K_i C_{OI} = K_3 C_{OI}$. The decomposition of ACET follows a series kinetics as follows (Eq. 7):

$$ACET \rightarrow OI \rightarrow CO_2 \quad (7)$$

The equation expressing the formation of organic intermediates is

$$r_{OI} = \frac{dC_{OI}}{dt} = \frac{K_1 C_{ACET}}{1 + K_2 C_{ACET} + K_3 C_{OI}} - \frac{K_4 C_{OI}}{1 + K_2 C_{ACET} + K_3 C_{OI}} \quad (8)$$

Finally, Eqs 9 and 10 predict the decomposition of ACET and the formation and consumption of OI; the estimated value of the constants K_1, K_2, K_3, and K_4 were estimated by nonlinear regression using the Levenberg–Marquardt equation with the use of Statistical 7.1 software.

$$-r_{ACET} = -\frac{dC_{ACET}}{dt} = \frac{0.025082 C_{ACET}}{1 + 0.001183 C_{ACET} + 0.0107 C_{OI}} \quad (9)$$

$$r_{OI} = \frac{dC_{OI}}{dt} = \frac{0.025082 C_{ACET}}{1 + 0.001183 C_{ACET} + 0.0107 C_{OI}} - \frac{0.009430 C_{OI}}{1 + 0.001183 C_{ACET} + 0.0107 C_{OI}} \quad (10)$$

whereK_1 - acetaminophen degradation reaction rate,K_2 - acetaminophen adsorption,K_3 - average adsorption, andK_4 - organic intermediate degradation reaction rate.

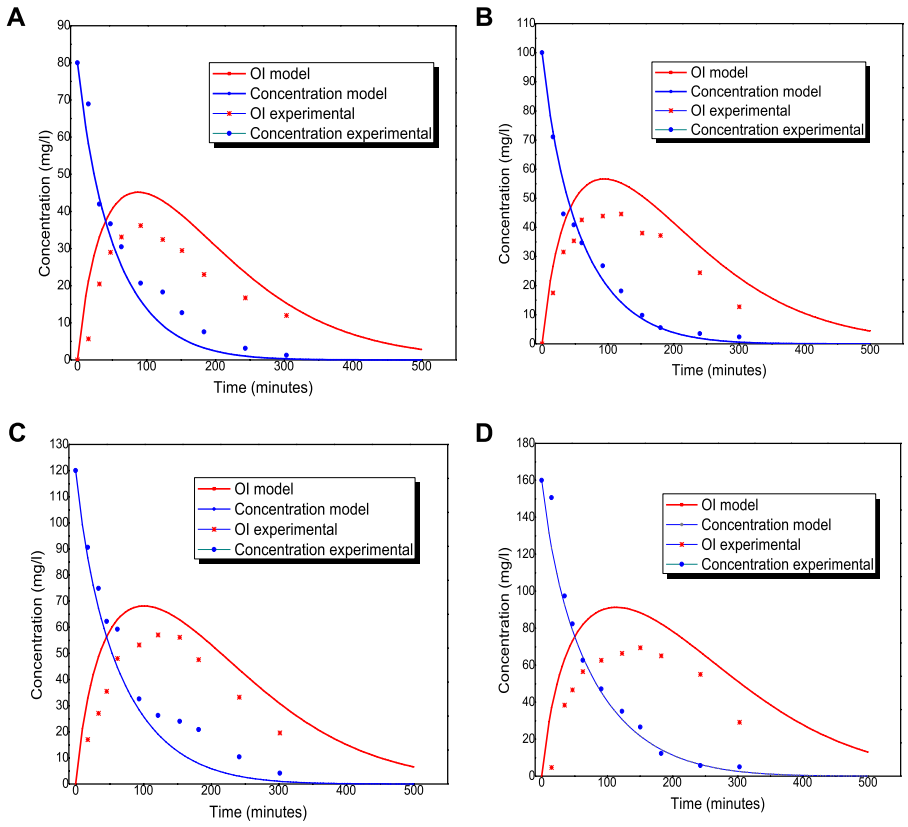

FIGURE 4
Result of the application of the LH-HW model predicting the decomposition of acetaminophen and the formation and consumption of organic intermediates, the continuous lines represent the model estimates and the points of the experimental data. **(A)** C_{ACET} = 80 mg/l, **(B)** C_{ACET} = 100 mg/l, **(C)** C_{ACET} = 120 mg/l, and **(D)** C_{ACET} = 160 mg/l.

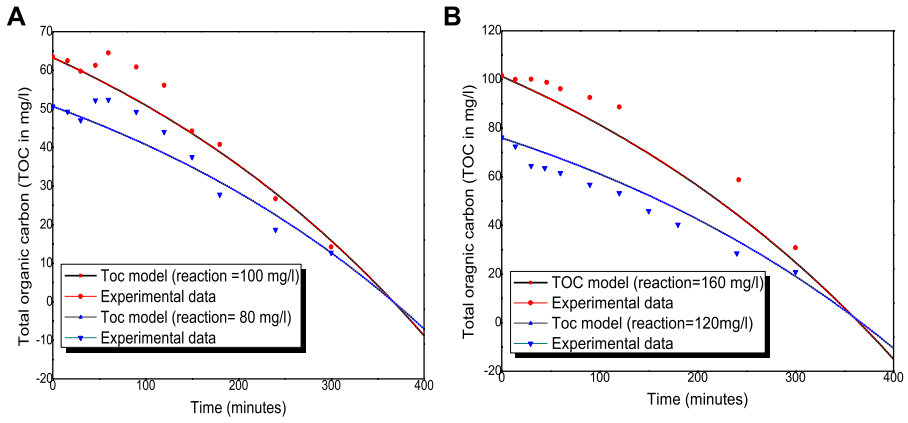

FIGURE 5
Behavior of the model is based on carbon TOC monitoring. In contrast to experimental data, the continuous lines represent the application of the model and the points of the experimental data. **(A)** Evaluation of the data of a reaction with a C_0 = 100 and 80 mg/l. **(B)** Evaluation of data from a reaction with a C_0 = 120 and 160 mg/l.

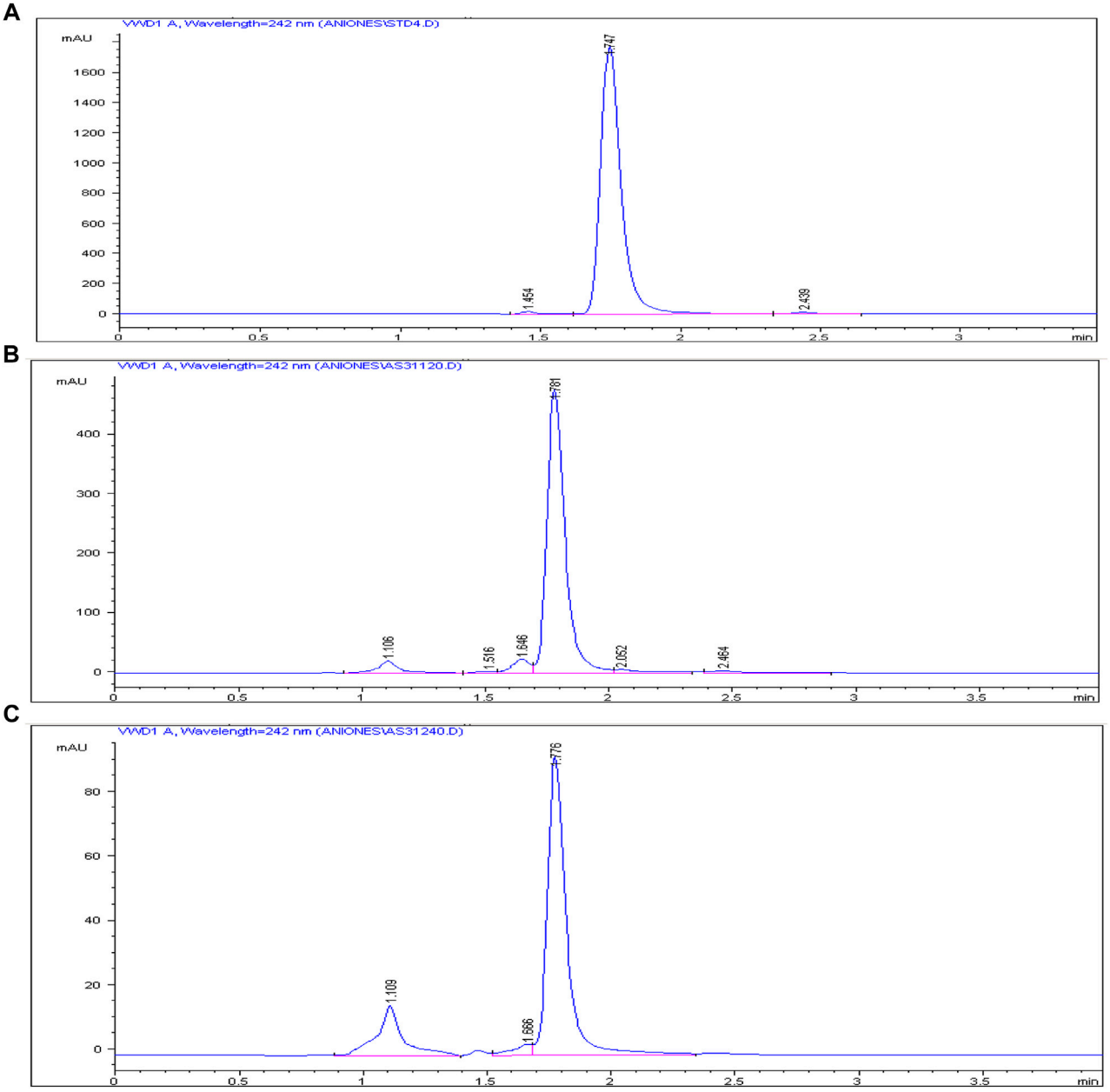

FIGURE 6
Profile of the qualitative identification of the organic intermediates in a sample of ACET with an initial concentration of 100 mg/l (mobile phase: 60% methanol; 40% water HPLC grade; injection flow: 0.8 ml/min, Zorbax C-18 column). **(A)** Initial sample of unreacted acetaminophen. **(B)** Chromatogram at 1 h of reaction. **(C)** Chromatogram at 2 h of reaction.

The experimental data of HPLC, TOC, and the OI generated by mass balance are shown in Figure 3.

With the estimated values of the kinetic constants, differential Eqs 9 and 10 were solved using Polymath 6.1 software. Figure 4 shows the results of the LH-HW model estimation in contrast with the experimental data.

Kinetic model based on total organic carbon

Zhang and Chuang (1999) suggest that the oxidation of organic compounds follows pseudo-first kinetics. These last authors studied the oxidation of nitroaromatics in an

industrial plant, suggesting total oxidation and partial oxidation reactions. The rate equation for the oxidation of the organic compound in the liquid phase in a Bach-type reactor can be expressed as follows with Eqs 11 and 12:

$$ACET + O_2 \rightarrow \quad CO_2 + H_2O \tag{11}$$

$$ACET + O_2 \rightarrow \quad OI + H_2O \tag{12}$$

The solutions are shown in Eqs 13 and 14.

$$ACET = \frac{ACET_0}{EXP\ (K_1 + K_2)t} \tag{13}$$

$$OI = \frac{K_2 ACET_0}{(K_1 + K_2)}\{1 - EXP[-(K_1 + K_2)t]\} \tag{14}$$

The conditions of the system of differential equations are at time t = 0; ACET = $ACET_0$ = TOC_0 and OI = 0 and at time t = t; ACET = ACET, OI = OI, and ACET + OI = TOC, where t - time, t = 0 - initial time, t = t - function at any time, $ACET_0$ - initial concentration of acetaminophen, K1, K2 - kinetic constants in min^{-1}, TOC_0 - initial concentration of total organic carbon, and OI - organic intermediates.

Combining the conditions

ACET + OIP = TOC and $ACET_0$ = TOC_0, expression 15 is obtained.

$$\frac{TOC}{TOC_0} = \frac{K_2}{K_1 + K_2} + \frac{K_1}{K_1 + K_2} EXP[-(K_1 + K_2)t]. \tag{15}$$

With this expression, the variation profile of TOC in a reaction can be predicted. Constants K_1 = 0.001735 min^{-1} and K_2 = 0.004037 min^{-1} were obtained from the experimental data using the Levenberg–Marquardt equation by nonlinear regression with the use of Statistical Software 7.1; the results are shown in Figure 5.

Identification of major organic intermediates

The results of ACET degradation show the formation and decomposition of different organic intermediates. To elucidate qualitatively and quantitatively by HPLC, the standard co-injection technique is performed. For this, the standards of 4-aminophenol (AP), hydroquinone (HQ), p-benzoquinone (BQ), and 1,2 dihydroxybenzene or catechol (CT) are injected after the ACET injections. For the comparison of the peaks detected in the ACET degradation samples, the retention times are checked, and the identified peaks are compared.

To determine the degradation pathway, 100 mg/l solutions of the standards are subjected to the degradation process under conditions similar to those of ACET and evaluated by HPLC. Based on these results, it is assumed that the degradation pathway

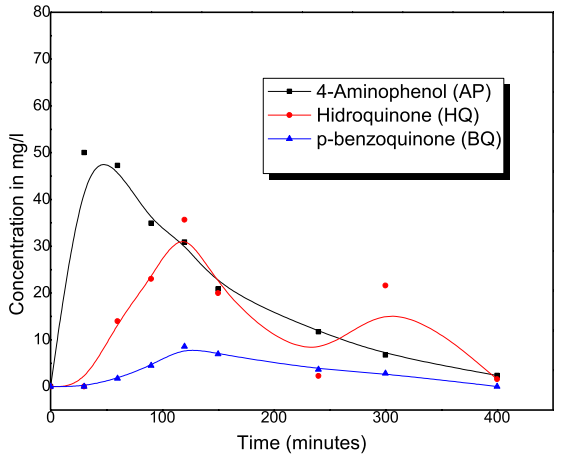

FIGURE 7
Profile of the distribution of formation and consumption of organic intermediates (OI) identified by liquid chromatography (HPLC) in degradation samples of acetaminophen. AP, HQ, and BQ profiles are observed.

is by hydroxylation and follows series kinetics. It is possible to consider as organic intermediates hydroxylated and nitro-aromatic species. The first reaction intermediate is AP (retention time = 2.162 min, injection volume 0.6 ml/min), followed by HQ (retention time = 1.109 and injection volume of 0.6 ml/min) and benzoquinone BQ (retention time = 1.66 min and injection volume of 0.8 ml/min). This last organic intermediate is formed by successive oxygenation in the reaction medium, and it is likely that from this component, fragmentation of the aromatic ring occurs, and structures with low carbon atoms are generated.

Figure 6 shows an HPLC chromatogram where the peaks of the intermediates are identified. Figure 7 shows the profiles of the intermediates identified under this analytical technique. CT is not a part of the ACET degradation pathway under the reaction conditions because hydroxyl radicals are not produced (in excess) to generate highly hydroxylated species such as 1,2-hydroxybenzene or 1,2,4-trihydroxybenzene. Under other procedures and with the addition of other oxidants such as H_2O_2 or O_3, if possible, as confirmed by Andreozzi et al. (2003), they used O_3/H_2O_2/UV to confirm that the intermediate products of the reaction are the result of ozone attack on the aromatic ring, forming highly hydroxylated species such as 1,2,4- trihydroxybenzene and 2- hydroxy-4-(N-acetyl-aminophenol).

Vogna et al. (2002) with the use of commercial catalysts showed the formation of 1-4 hydroquinone, 4-acetylaminocatechol and fragments of acetic acid, oxalic acid,

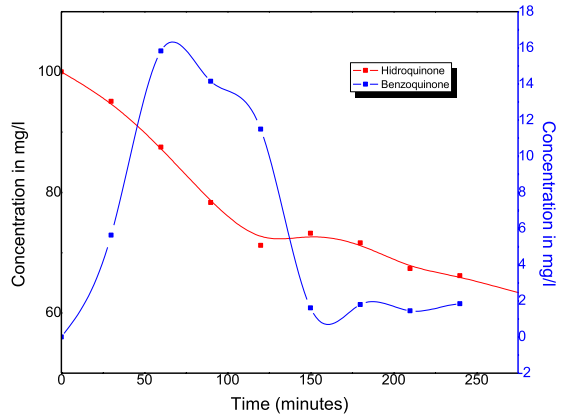

FIGURE 8
Profile of the distribution of formation and consumption of organic intermediates (OI) identified by liquid chromatography (HPLC) in HQ degradation samples.

and formic acid. Yang et al. (2008) and Yang et al. (2010) confirmed that the final oxidation products are low molecular weight structures of at least four carbon atoms.

TABLE 1 Intermediate organic compounds detected in samples of photocatalytic degradation of ACET.

m/z ratio	Retention time (min)	Identified component
110	12.84	Hydroquinone
256	20.87	Hexadenoic acid

Our study shows the formation of relatively stable species with the use of silver-doped anatase powders, without using commercial catalysts (which are made up of the anatase and rutile phases). There is no evidence of the formation of highly hydroxylated species.

In Figure 8, the degradation profile of the HQ standard is shown, which degrades under the formation of BQ, the last major intermediate determined under HPLC. The calibration curves of the intermediates are injected in a concentration range of 0–100 mg/l.

ACET reaction samples (200 mg/l) were treated by solid-phase microextraction with LiChrolut® EN extraction cartridges; the organic phase extracts were analyzed by GC-MS for

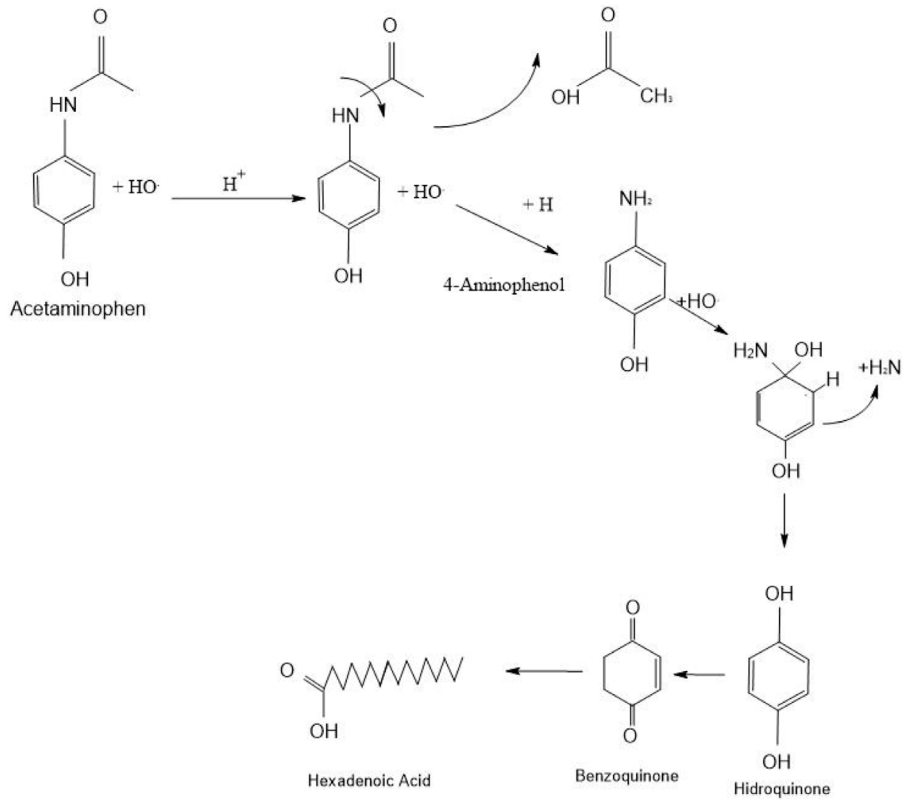

FIGURE 9
Major organic intermediates identified in the acetaminophen transformation pathway with TiO_2-Ag catalysts synthesized by the sol–gel method, where the predominant phase is anatase. Under the following reaction conditions: reaction volume: 250 ml, catalyst mass = 2 g/l, four commercial visible light lamps were irradiated.

confirmation and detection of other minor intermediaries. The results are shown in Table 1.

Based on the results observed, it is proposed that the initial degradation pathway of acetaminophen is as follows (Figure 9).

Conclusion

The synthesis of the catalyst by the sol–gel method promoted the formation of the crystalline phase of anatase. The silver deposited as metallic particles on the catalyst by photo-deposition promotes changes in the surface of the semiconductor that make it active in visible light; the amount of 1.17% by weight of metallic silver deposited is sufficient to consider a material capable of removing more than 80% of the initial concentration of acetaminophen under the action of visible light.

The reaction kinetics has a trend similar to that of a first-order reaction. Under the LH-HW model, the process is assumed to be a series reaction, the estimated kinetic constants suggest that at the beginning of the reaction, the rate is similar to the adsorption constant. As the reaction proceeds, the rate of formation and decomposition of the intermediates is minor than that of the original molecule, and adsorption processes dominate the behavior of the intermediates.

The experimental results fit the model of LH-HW. Additionally, the models based on the behavior of carbon suggest slow mineralization processes due to the formation of organic intermediates that remain within the reaction; these major intermediates were identified with liquid chromatography techniques and by co-injection of standards; the first intermediate formed is 4-aminophenol, a product of successive hydroxylation and oxygenation, which degrades into hydroquinone by para-substitution of the nitrogenous group by a hydroxyl group and the subsequent removal of the functional group containing the nitrogen.

Successive oxygenation in the reaction medium promotes the generation of 1,4-benzoquinone by oxidation of 1,4-dihydroxybenzene or hydroquinone. From this intermediate organic compound, it is possible that the aromatic ring is fragmented, generating species such as carboxylic acids, esters, or compounds containing the carbonyl group (C=O), as well as nitrates and nitrites derived from the oxidation of the nitrogenous groups that remain in reaction.

Finally, it can be concluded that the synthesized material is efficient for the removal of this model component and that the major intermediates detected are products of the hydroxylation processes.

Data availability statement

The raw data supporting the conclusion of this article will be made available by the authors, without undue reservation.

Author contributions

CA and AdC conceived and planned the experiments. All authors provided critical feedback and helped shape the research, analysis, and manuscript. All authors have read and agreed to the published version of the manuscript.

Acknowledgments

The authors are grateful to SO (Autonomous Metropolitan University) for their assistance in X-ray diffraction (DRX) and energy dispersive X-ray fluorescence (EDXRF).

Conflict of interest

The authors declare that the research was conducted in the absence of any commercial or financial relationships that could be construed as a potential conflict of interest.

Publisher's note

References

Abbas, H., Vannier, R. N., Mahmoud, T., and Jamil, T. S. (2022). Improving of photocatalytic activity of barium ferrate via bismuth and copper co-doping for degradation of paracetamol under visible light irradiation. *J. Environ. Sci.* 112, 331–342. doi:10.1016/j.jes.2021.05.008

Aguilar, C. A., Montalvo, C., Zermeño, B., Ceron, R. M., Cerón, J. G., Anguebes, F., et al. (2019). Photocatalytic degradation od acetaminophen, tergitol and nonylphenol with catalysts TiO_2/Ag under UV and Vis light. *Int. J. Environ. Sci. Technol.* 16, 843–852. doi:10.1007/s13762-018-1707-x

Al-Gharibi, M. A., Kyaw, H. H., Al-Sabahi, J. N., Myint, M. T. Z., Al-Sharji, Z. A., and Al-Abri, M. Z. (2021). Silver nanoparticles decorated zinc oxide nanorods supported catalyst for photocatalytic degradation of paracetamol. *Mat. Sci. Semicond. process.* 134, 105994. doi:10.1016/j.mssp.2021.105994

Aminzadeh, H., Mohaddeseh, S., Iman, M., and Hassan, S. (2021). Assembly of CuO nanorods onto poly(glycidylmethacrylate)@polyaniline core–shell microspheres: Photocatalytic degradation of paracetamol. *Appl. Organomet. Chem.* 35, 1–12. doi:10.1002/aoc.6423

Andreozzi, R., Caprio, V., Marotta, R., and Vogna, D. (2003). Paracetamol oxidation from aqueous solutions by means of ozonation and H_2O_2/UV system. *Water Res.* 37, 993–1004. doi:10.1016/s0043-1354(02)00460-8

Bavasso, I., Poggi, C., and Elisabetta, P. (2020). Enhanced degradation of paracetamol by combining UV with electrogenerated hydrogen peroxide and ozone. *J. Water Process Eng.* 34, 101102. doi:10.1016/j.jwpe.2019.101102

Bedner, M., and Maccrehan, W. (2006). Transformation of acetaminophen by chlorination produces the toxicants 1, 4-benzoquinone and *N*-Acetyl-*p*-benzoquinone imine. *Environ. Sci. Technol.* 40, 516–522. doi:10.1021/es0509073

Behpour, M., Ghoreishi, S. M., and Razavi, S. (2010). Photocatalytic activity of TiO_2/Ag nanoparticle on degradation of water pollutions. *Dig. J. Nano. Mat. Bios.* 5, 467–475.

Benssassi, M. E., Lamia, M., Khouloud, T., Bouchra, L., Thajar, S., Santaballa, J. A., et al. (2021). Removal of paracetamol in the presence of iron(III) complexes of glutamic and lactic acid in aqueous solution under NUV irradiation. *Sep. Purif. Technol.* 261, 118195. doi:10.1016/j.seppur.2020.118195

Borras-Ferrís, J., Sánchez-Tovar, R., Blasco-Tamarit, E., Muñoz-Portero, M. J., Fernández-Domene, R. M., and García-Antón, J. (2019). TiO_2 nanostructures for photoelectrocatalytic degradation of acetaminophen. *Nanomaterials* 9, 583. doi:10.3390/nano9040583

Castro, L. I., Baños, M. I., CastroLópez, M. A., and Torres, B. L. (2015). Ecofarmacovigilancia en México: Perspectivas para su implementación. *Rev. Mex. Cienc. Farm.* 46, 16–40.

Chan, R., Chart, C., Wilai, C., Alongkot, B., and Phitsanu, T. (2022). Ocurrence of antibiotics in typical pig farming and its wasterwater treatment in Thailand. *Emerg. Contam.* 8, 21–29. doi:10.1016/j.emcon.2021.12.003

Chang, C.-T., Wang, J.-J., Oyang, T., Zhang, Q., and Jing, Y.-H. (2015). Photocatalytic degradation of acetaminophen in aqueous solutions by TiO_2/ZSM-5 zeolite with low energy irradiation. *Mater. Sci. Eng. B* 196, 53–60. doi:10.1016/j.mseb.2014.12.025

Chopra, S., and Kumar, D. (2020). Biodegradation and kinetic analysis of acetaminophen with co-culture of bacterial strains isolated from Sewage wastewater. *Curr. Microbiol.* 77, 3147–3157. doi:10.1007/s00284-020-02137-6

Dibene, K., Idris, Y., Salima, A., Lamia, K., Abdeltif, A., and Farida, A. B. (2021). Central composite design applied to paracetamol degradation by heat-activated peroxydisulfate oxidation process and its relevance as a pretreatment prior to a biological treatment. *Environ. Technol.* 42, 905–913. doi:10.1080/09593330.2019.1649308

García-López, E., Giuseppe, M., and Palmisano, L. (2019). Chapter 5 - photocatalytic and catalytic reactions in gas–solid and in liquid–solid systems, Editor(s): G. Marcì and L. Palmisano, *Heterogeneous photocatalysis*. Italia: Elsevier, 153–176. doi:10.1016/B978-0-444-64015-4.00005-5

Gomez-Solís, C., Mendoza, R., Rios-Orihuela, J. F., Robledo-Trujillo, G., Diaz-Torres, L. A., Oliva, J., et al. (2021). Efficient solar removal of acetaminophen contaminant from water using flexible graphene composites functionalized with Ni@TiO2:W nanoparticles. *J. Environ. Manage.* 290, 112665. doi:10.1016/j.jenvman.2021.112665

Guo, Q., Chuanyao, Z., Zhibo, M., and Xueming, Y. (2019). Fundamentals of TiO_2 photocatalysis: Concepts, mechanisms, and challenges. *Adv. Mat.* 31 (50), e1901997. doi:10.1002/adma.201901997

Hernández, L. A., Rakesh, S., Rojas-Trigos, J. B., Marín, E., and Garcia, C. D. (2021). Monitoring the advanced oxidation of paracetamol using ZnO films via capillary electrophoresis. *J. Water Process Eng.* 41, 102051. doi:10.1016/j.jwpe.2021.102051

Hurtado, L., Romero, R., Mendoza, A., Brewer, S., Donkor, K., Gómez, R., et al. (2019). Paracetamol mineralization by Photo Fenton process catalyzed by a Cu/Fe-PILC under circumneutral pH conditions. *J. Photochem. Photobiol. A Chem.* 373, 162–170. doi:10.1016/j.jphotochem.2019.01.012

Jallouli, N., Kais, E., Hassen, T., and Mohamed, K. (2017). Photocatalytic degradation of paracetamol on TiO_2 nanoparticles and TiO_2/cellulosic fiber under UV and sunlight irradiation. *Arab. J. Chem.* 10, S3640–S3645. doi:10.1016/j.arabjc.2014.03.014

Jannatun, Z., and Ufana, R. (2020). Microwave-assisted degradation of paracetamol drug using polythiophene-sensitized Ag–Ag_2O heterogeneous photocatalyst derived from plant extract. *ACS Omega* 5 (27), 16386–16394. doi:10.1021/acsomega.0c00405

Janus, M., and Morawski, A. W. (2007). New method of improving photocatalytic activity of commercial Degussa P25 for azo dyes decomposition. *Appl. Catal. B Environ.* 75, 118–123. doi:10.1016/j.apcatb.2007.04.003

Kabra, K., Chuadhary, R., and Sawhney, R. L. (2004). Treatment of hazardous organic and inorganic compounds through aqueous-phase. Photocatalyst: A review. *Ind. Eng. Chem.* 43, 7683–7696. doi:10.1021/ie0498551

Kőrösi, L., Szilvia, P., Ménesi, J., Erzsébet, I., Volker, Z., André, R., et al. (2008). Photocatalytic activity of silver-modified titanium dioxide at solid–liquid and solid–gas interfaces. *Colloids Surfaces A Physicochem. Eng. Aspects* 319, 136–142. doi:10.1016/j.colsurfa.2007.11.030

Kumari, S., and Naresh, K. (2021). River water treatment using electrocoagulation for removal of acetaminophen and natural organic matter. *Chemosphere* 273, 128571. doi:10.1016/j.chemosphere.2020.128571

Moma, J., and Baloyi, J. (2018). "Modified titanium dioxide for photocatalytic applications," in *Photocatalysts - applications and attributes*. Editors S. B. Khan and K. Akhtar (London: IntechOpen). doi:10.5772/intechopen.79374

Seery, M. K., Reenamole, G., Floris, P., and Pillai, S. C. (2007). Silver doped titanium dioxide nanomaterials for enhanced visible light photocatalysis. *J. Photochem. Photobiol. A Chem.* 189, 258–263. doi:10.1016/j.jphotochem.2007.02.010

Vogna, D., Marotta, R., Napolitano, A., and d´Ischia, M. (2002). Advanced Oxidation Chemistry of Paracetamol, UV/H_2O_2 induced hidroxilation/degradation pathways and ^{15}N-aided inventory of nitrogenous breakdown products. *J. Org. Chem.* 67, 6143–6151. doi:10.1021/jo025604v

Wahyuni, E. T., and Roto, R. (2018). "Silver nanoparticle incorporated titanium oxide for bacterial inactivation and dye degradation," in *Titanium dioxide - material for a sustainable environment*. Editor D. Yang (London: IntechOpen). doi:10.5772/intechopen.75918

Wilkinson, J. L., Alistair, B. A., Kolpin, D. W., Kenneth, M. Y., Racliffe, W. S., Galbán-Malagón, C., et al. (2022). Pharmaceutical pollution of the world's rivers. *Proc. Natl. Acad. Sci. U. S. A.* 119 (8), e2113947119. doi:10.1073/pnas.2113947119

Yang, L., Liya, E., and Ray, M. (2008). Degradation of paracetamol in aqueous solutions by TiO_2 photocatalysis. *Water Res.* 42, 3480–3488. doi:10.1016/j.watres.2008.04.023

Yang, L., Yu, L., and Ray, M. (2010). Photocatalytic oxidation of paracetamol: Dominant reactants, intermediates, and reaction mechanisms. *Environ. Sci. Technol.* 43, 460–465. doi:10.1021/es8020099

Yong, M. D., Chen-Yin, L., Wei-Ho, T., and Jih-Mirn, J. (2022). Plasmon Ag/$AgVO_3$/TiO_2-nanowires S-scheme heterojunction photocatalyst for CO_2 reduction. *J. Environ. Chem. Eng.* 10, 108045. doi:10.1016/j.jece.2022.108045

Zhang, Q., and Chuang, K. T. (1999). Lumped kinetic model for catalytic wet oxidation of organic compounds in industrial wastewater. *AIChE J.* 45, 145–150. doi:10.1002/aic.690450112

Ziylan-Yavaş, A., and Ince, N. H. (2016). Enhanced photo-degradation of paracetamol on n-platinum-loaded TiO_2: The effect of ultrasound and OH/hole scavengers. *Chemosphere* 162, 324–332. doi:10.1016/j.chemosphere.2016.07.090